

Testicular Changes of Honey Bee Drones, *Apis mellifera* (Hymenoptera: Apidae), During Sexual Maturation

Colby D. Klein,^{1,3,*} Ivanna V. Kozii,¹ Sarah C. Wood,¹ Roman V. Koziy,¹
Michael W. Zabrodski,¹ Ihor Dvylyuk,¹ Igor Medici de Mattos,¹ Igor Moshynskyy,¹
Ali Honaramooz,^{2,*} and Elemir Simko¹

¹Department of Veterinary Pathology, Western College of Veterinary Medicine, University of Saskatchewan, 52 Campus Drive, Saskatoon, SK S7N 5B4, Canada, ²Veterinary Biomedical Sciences, Western College of Veterinary Medicine, University of Saskatchewan, 52 Campus Drive, Saskatoon, SK, S7N 5B4, Canada, and ³Corresponding author, e-mail: colby.klein@usask.ca

Subject Editor: Hongmei Li-Byarlay

Received 28 April 2021; Editorial decision 20 June 2021

Abstract

The normal developmental anatomy and histology of the reproductive tract of the honey bee drone, *Apis mellifera* (Linnaeus, 1758), has been well documented. The post-emergence maturation changes of the accessory glands are likewise well understood, but the normal histological changes of the testicle undergoing physiologic atrophy are not well characterized. To address this knowledge gap, herein we describe the anatomy and sequential histological stages of normal testicular atrophy of drones sampled daily from emergence to sexual maturity in the spring (June) and early summer (July). Testicular histological changes during maturation are characterized by the following stages: I) conclusion of spermiogenesis; II) evacuation of spermatodesms from tubular lumens; III) progressive follicular cell atrophy, and IV) complete atrophy and collapse of testicular parenchyma. Tubular changes occur in a basilar to apical direction where segments closer to the vas deferens are histologically more mature than corresponding apical segments. In addition, the rate of testicular maturation was found to change with seasonal progression. This description of physiologic testicular atrophy should be useful for future studies investigating potential pathological effects of stressors on drone testes during sexual maturation.

Key words: drone, histology, maturation, testicle, reproduction

The reproductive anatomy of the male honey bee was first described and illustrated by the naturalist Jan Swammerdam in the posthumous publication *Biblia Naturæ* (Swammerdam 1738). Drone reproductive organs consist of paired testes, conducting tubules and ducts (vas efferens, vas deferens, and ejaculatory ducts), accessory sex glands (seminal vesicles and mucus glands), and endophallus (Bishop 1920). Subsequent studies described the macroscopic and microscopic structures of reproductive organs in developing brood and maturing adult drones (Zander 1916, Snodgrass and Morse 1956, Woyke and Ruttner 1958; Moors et al. 2005, 2012, Moors and Billen 2009, Lago et al. 2020).

Developmental anatomy (Zander 1916) and histology (Snodgrass 1910, Zander 1916, Bishop 1920, Snodgrass and Morse 1956, Woyke and Ruttner 1958) of drone testes during larval and pupal stages have been described previously, and Lago et al (Lago et al. 2020) recently published a histological atlas that thoroughly depicts spermatogenesis and testicular development of drones prior to emergence. The functional units of the insect testis are the testicular tubules (Snodgrass 1935, Snodgrass and Morse 1956) [also called testicular follicles or sperm-tubes (Snodgrass 2018)].

Hundreds of tubules radiate out from the vas deferens, via individual vas efferens (Snodgrass 2018) continuous with the basilar tubule, and extend to the blind-ended (apical) tubule at the periphery of the testicle (Lago et al. 2020). All testicular tubules are already present at the early larval stage (Zander 1916, Lago et al. 2020). Rapid testicular growth is due to elongation of the testicular tubules along the apical–basal axis by mitotic divisions of the spermatogonia, which eventually form germ cell clusters (late larval stage) and undergo meiosis (in pupae after capping), which generates spermatids in red-eyed pupae. Spermiogenesis occurs at the final pupal (or also called pharate adult) stage during which all spermatozoa are produced from spermatids before the emergence of adult drones (Lago et al. 2020).

Individual testicular tubules are surrounded by an inner peritoneal sheath (Lago et al. 2020) that contains follicular cells (Da Cruz-Landim et al. 1980, Power et al. 2020) [also called nutritive (Moors et al. 2009), or cyst cells (Snodgrass and Morse 1956, Cruz-Landim 2001)], which house and support the developing gametes in specialized intracellular cavities (Snodgrass 1935). The entire testis is also surrounded by a peritoneal sheath (Snodgrass 1935) [or

testicular capsule (Forbes 1954, Kapil 1962)]. The apical ends of the testicular tubules are located along the outer periphery adjacent to the peritoneum (apical surface of testes), and the basilar portions of testicular tubules oriented centro-medially are adjacent to the vas deferens. These tubules are arranged similar to the vesicles of an orange segment, radiating outwards from the vas deferens. Numerous tracheoles infiltrate the capsule and extend between the testicular tubules (Klowden 2013) providing gas exchange.

The most differentiated (older) germ cells are found at the basilar segments of testicular tubules (Snodgrass 1935, Lago et al. 2020). The germ cells continue spermatogenesis within the follicular cells, progressively forming spermatogonia, spermatocytes, spermatids, and spermatozoa defining the histological zones of growth, maturation, and transformation respectively (Smith 1968). The distinct zones can be observed simultaneously during active spermatogenesis (Rego et al. 2013), but in emergent drones only the final stage may be observed histologically (Snodgrass 1910). The mature spermatozoa are bundled together [forming spermatodesms (Smith 1968)] and rupture free from the follicular cell into the follicular lumen and progress towards vas efferens and common vas deferens. The process of germ cell generation and meiosis is reported to be completed by the sixth day of pupal development (Bishop 1920, Snodgrass and Morse 1956) when the testes are most developed, occupying the majority of the abdomen. The resulting testes no longer have tubules undergoing active elongation (germ cell generation and meiosis), and predominantly display spermiogenesis (the final stage of spermatogenesis), which is maintained until emergence (Lago et al. 2020). In tubules undergoing spermiogenesis, we can see the conversion of spermatids to spermatozoa, which are then bundled together and released into the paired vas deferens and seminal vesicles over the first few days of life (Bishop 1920).

The developmental larval and pupal anatomy and histology of the accessory sex glands have been described in detail from the first larval instar to emergence (Zander 1916, Bishop 1920; Moors et al. 2005, 2012, Moors and Billen 2009). The seminal vesicles are enlarged segments of the vasa deferentia and the majority of their growth is completed by 18 d postoviposition (Zander 1916). The seminal vesicles begin producing and storing secretions as early as day 20 postoviposition and begin receiving sperm from the testes several days before emergence (Bishop 1920). The mucus glands, ejaculatory duct, and endophallus begin to take their final morphology and anatomical position approximately 1 wk before emergence (Zander 1916).

After emergence, the reproductive organs of drones continue to develop and undergo rapid changes during their sexual maturation (6 to 12 d postemergence). The gross and histological changes to the vas deferens, seminal vesicles, mucus glands, and endophallus during sexual maturation have been described very well (Bishop 1920, Woyke and Ruttner 1958, Woyke and Jasinski 1978, Colonello and Hartfelder 2005; Moors et al. 2005, 2012, Moors and Billen 2009). Sperm produced in the testes is transferred to the seminal vesicles via the proximal vas deferens from 3 to 8 d postemergence (Bishop 1920, Jaycox 1961) where they remain within the seminal fluid until ejaculation (Collins et al. 2006). The heads of the spermatozoa are imbedded into the luminal surface of the epithelium of seminal vesicles where they complete their final portion of development (Bishop 1920, Snodgrass and Morse 1956). The inner circumferential and outer longitudinal muscle layers are responsible for expelling the contents of the seminal vesicles along a short distal vas deferens to the

mucus gland and ejaculatory duct during intromission (Snodgrass and Morse 1956). The mucus glands gradually enlarge and accumulate secretions for the first nine days after emergence and their function and histological development has been described previously (Bishop 1920, Colonello and Hartfelder 2003, Moors et al. 2005). The mucus glands are lined by a simple glandular and secretory columnar epithelium, surrounded by three muscular layers (inner longitudinal, middle circumferential, and outer longitudinal layers) (Bishop 1920) which contract simultaneously with muscles of seminal vesicles during copulation and forcefully eject the contents of the seminal vesicles and mucus glands through the common ejaculatory duct to the endophallus (Woyke and Ruttner 1958).

The endophallus is divided into three portions: the vestibulum, the neck (cervix), and the bulb, which have been described anatomically and histologically in detail (Bishop 1920, Snodgrass and Morse 1956, Moors and Billen 2009, Moors et al. 2012). During ejaculation, the forceful contraction of the drone abdominal muscles forces the distal reproductive organ to evert and eviscerates the drone while achieving full eversion of the penis.

Postemergence testicular changes are remarkable during the sexual maturation of drones. The testes of newly emerged drones release mature spermatodesms to be stored in the seminal vesicles over the first few days of life (Bishop 1920) and subsequently undergo rapid involution and marked reduction in size (Snodgrass 1910). Drones reach sexual maturity 6–12 d postemergence, at which time the testes are reduced to a fraction of their original size (Snodgrass 1910, Bishop 1920, Woyke and Ruttner 1958, Landim 2008). This marked testicular size reduction is an indicator of the functional maturity of drones (Bishop 1920). Chronological testicular involution has been described histologically in several Hymenopteran species [wasps (Moors et al. 2009), ants (Forbes 1954, Shyamalanath and Forbes 1983, Ball and Vinson 1984, Allard et al. 2011), and other bee species (Cruz-Landim and Dallacqua 2002, Sawarkar and Tembhare 2015)]; however, a detailed histological description of chronological testicular involution during sexual maturation of drones is still lacking.

Accordingly, the purpose of this study was to create a histological atlas of chronological changes associated with testicular involution during sexual maturation of experimental drones with synchronized age from day 1 to 21 postemergence.

Materials and Methods

Experimental Colonies

Research colonies originated from blended local commercial beekeeping stock with a minor contribution of New Zealand packaged bees that were cross-bred and represented a genetic mixture most closely resembling *Apis mellifera carnica*. The colonies were located at the University of Saskatchewan Research Apiary (52°07'38.4"N 106°36'35.6"W) in the city of Saskatoon, Saskatchewan, Canada. Prior to the experiment, colonies at the apiary received standard spring treatments (as practised in Western Canada) of amitraz (Ampar. Veto-Pharma, France) and oxytetracycline-HCl (Oxytet-25. Medivet Pharmaceuticals, Canada) according to label instructions. One strong and healthy colony with a one-year-old (marked) queen was selected and fed ad libitum 1:1 (w:w) sugar syrup and pollen patty (Ultra Bee Patties, Mann Lake Ltd., Hackensack, MN) to facilitate early spring build-up until the initiation of the trial in May 2017.

Design of Experimental Hive

The selected experimental colony was housed in a standard 10-frame Langstroth hive with two brood chambers and additional honey supers added as needed during the honey flow. A drone compartment was built using queen excluder mesh in the top brood chamber (Fig. 1). Accordingly, the experimental hive was divided into three compartments: 1) a brood chamber containing 16 frames (10 in the bottom, 6 in the top brood chamber), 2) a drone compartment adjacent to a side wall containing 3 frames (one drone, one open worker brood, and one honey and pollen frame in positions 3, 2, and 1, respectively (Fig. 1), and 3) one or more honey supers separated from the brood chambers by a queen excluder.

Rearing and Sampling Experimental Drones

To raise drones with synchronized age, the queen was caged for 24 h in the drone compartment containing a plastic drone frame (Pierco, Riverside, CA) with drawn-out wax foundation, a frame with open worker brood, and a honey and pollen frame (Fig. 1). After 24 h of laying eggs on the drone frame, the queen was transferred back to the brood chamber while the drone frame remained within the drone compartment. At day 21 postoviposition, all bees were removed from the drone compartment to exclude any potential nonexperimental drones. To track the emergence date of experimental drones, the drone compartment was inspected daily from day 23 to 26 postoviposition to mark all emerged drones during past 24 h with a specific color for that day using a queen marking pen. The emerged drones remained entrapped within the drone compartment for the entire duration of the experiment (from day 1 to day 21 postemergence). To evaluate daily sequential chronological testicular changes during sexual maturation of drones, 10 marked drones of the same age were collected each morning (6:00–7:00 a.m. during low flight intensity) for three weeks postemergence. Drones were collected into chilled (6°C) buffered 10% formalin to reduce the risk of everting the endophallus as they became mature. This experiment was performed in June and then repeated in July 2017.

Macroscopic Evaluation of Testes During Sexual Maturation

Macroscopic morphological changes of drone's reproductive organs were assessed by dissection ($n = 3$ per day of age in June and July) of formalin-fixed drones under a stereomicroscope (Olympus-SZ61, Japan) and by photography (Olympus DP71 microscope digital camera – Olympus, Japan) using 10–15 consecutive field depths (Fig. 2A and B). The digital images were stacked with Helicon Focus 6.7.1. (Helicon Soft Ltd., Ukraine) to obtain a full depth in-focus image. Sexual maturation was assessed using the (coronal) 2D surface area of the testes measured by an image analysis software (Image-Pro Premiere 9.1 software, Media Cybernetics, Rockville, MD).

Microscopic Evaluation of Testes During Sexual Maturation

Microscopic evaluation of testes from 6 drones of the same age per day (day 1 to 21 postemergence) was performed for experiments in June and July. A dorsal incision was made along the abdomen 24 h after drone collection in formalin, to enhance penetration and fixation for at least 48 h before further processing. To preserve the in-situ orientation of the reproductive organs, the intact (undissected) formalin-fixed abdomens were subjected to a standard histological tissue processing for mammalian species. Briefly, the formalin-fixed abdomens were dehydrated in

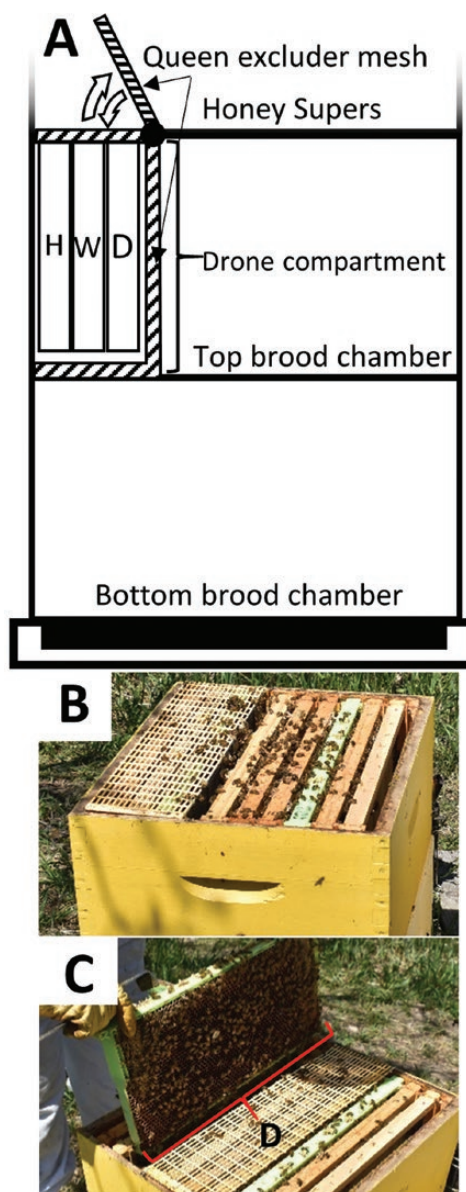


Fig. 1. Schematic diagram (A) and photographs (B and C) of experimental hive used in this study. Three-frame drone compartment was built using plastic queen excluder mesh in the top brood chamber. A honey and pollen (H), open worker brood (W), and experimental drone (D) frame with drawn wax foundation were placed in the first, second, and third positions, respectively. Newly emerged drones were marked with a specific color for each day using a queen marking pen. (B) Closed drone compartment where drones matured into adulthood; (C) Open drone compartment with a green drone frame (D) during inspection and marking of newly emerged drones on days 23, 24, 25, 26 postoviposition.

progressive alcohol baths (70, 80, 95, 100%) for one hour in each concentration, then transferred to xylene for one hour before being exposed to 60°C paraffin under a vacuum. To reduce sectioning artifact, the dorsal abdominal cuticle was removed from paraffinized abdomens under a dissecting microscope with heated tools, and subsequently the whole abdomens were embedded dorsoventrally in paraffin blocks (Paraplast Plus, Leica Biosystems, Richmond, IL) to allow dorsal aspects of the abdomen to be sectioned first. Serial coronal abdominal sectioning (5 μ m thick) was performed until medial coronal gonadal sections

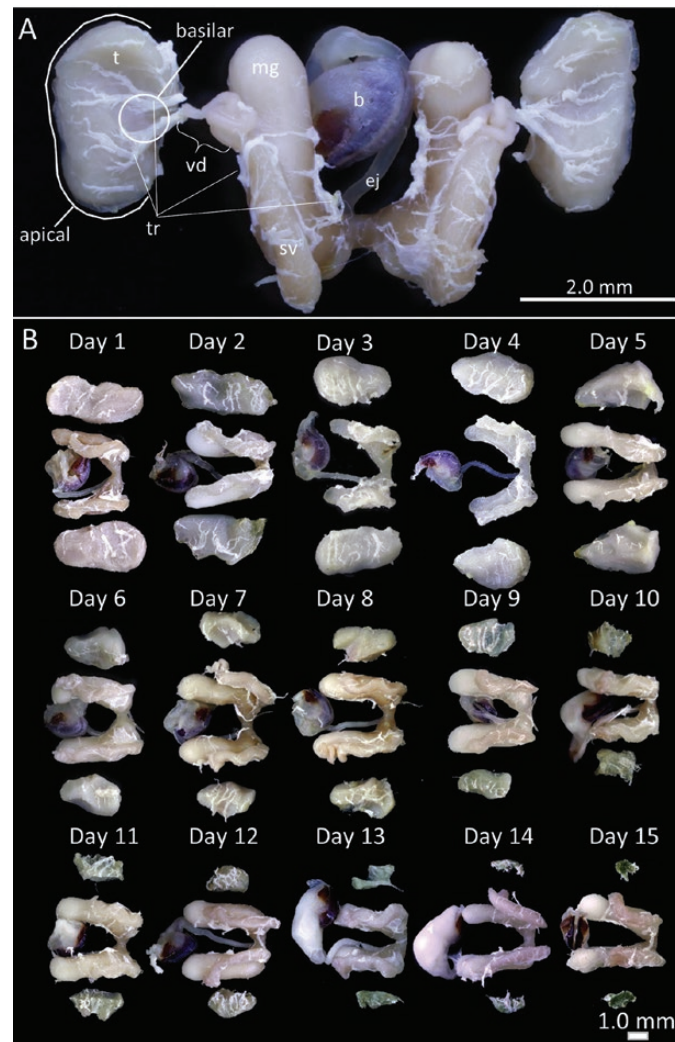


Fig. 2. Dissected drone reproductive tract after formalin fixation. (A) Dissected reproductive tract of immature drone (day 7): b, bulbus; ej, ejaculatory duct; mg, mucous gland; sv, seminal vesicle; t, testicle; tr, tracheal network. (B) Dissected reproductive tract from emergence (day 1) to sexual maturity (day 15) of representative drones. The testes are at their greatest size at emergence and gradually involute to the end-stage testes once sexual maturation is reached.

with maximal coronal-sectional area were obtained, which were mounted on glass slides, dried for 1 h at 65°C, and stained with a standard histological hematoxylin and eosin (H&E) stain following the previously published procedure (Suvarna et al. 2012). Briefly, xylene 2 min, xylene 2 min, 100% ethyl alcohol 2 min, 100% ethyl alcohol 2 min, 90% ethyl alcohol 2 min, 70% ethyl alcohol 2 min, running 40°C water 1 min, Surgipath Harris hematoxylin 560 (Leica Biosystems, Richmond, IL) 5 min, running 40°C water 1 min, 0.3% acid alcohol 15 s, running 40°C water 1 min, Surgipath blue buffer 8 (Leica Biosystems, Richmond, IL) 1 min, running 40°C water 3 min, 80% ethyl alcohol 1 min, Surgipath alcoholic eosin 515 Y (1%) (Leica Biosystems, Richmond, IL) 30 s, 90% ethyl alcohol 1 min, 90% ethyl alcohol 1 min, 100% ethyl alcohol 15 s, 100% ethyl alcohol 15 s, 100% ethyl alcohol 15 s, xylene 2 min, xylene 1 min, xylene 1 min. The slides were then cover slipped in a fume hood using Micromount (Leica Biosystems, Richmond, IL) (Luna and Pathology (U.S.) 1968).

The H&E-stained tissue sections were evaluated by light microscopy; microscopic changes were described for each day and histologic images were captured under various magnifications using an Olympus BX51 microscope and Olympus DP71 microscope

digital camera. Microscopic evaluation was focused on the testicular parenchyma (germ cells, tubular follicular and epithelial cells) and supporting testicular structures (visceral fat body, tracheal mesh, and peritoneum). Testicular changes during the sexual maturation period were divided into four distinct stages that were described histologically.

Daily Temperature

Daily mean temperature data were collected from publicly accessible historical weather data (Meteorological Station: Saskatoon Rcs, SK, Canada) (Government of Canada, 2011) from June to July and compared to sexual maturation length and period of drones evaluated in experiments performed in June and July, 2017.

Analysis of Data

Sexual maturation period was evaluated by testicular involution measured by 2D testicular surface. For each drone, the 2D surface area was added for both testes ($n = 3$ drones per day) and plotted against the age of the drone for both experiments performed in June and July. The total testicular surface areas were compared between the two experiments using one-way ANOVA comparing the

gonad size on each day of maturation between the two months with STATA-15 (College Station, TX) statistical analysis software.

Histological changes in testes were described for 6 drones for each day between day 1 and 21 postemergence (in June and July), which were subsequently grouped into 4 testicular maturation stages based on common progressive changes in testicular involution during sexual maturation of drones.

Results

Macroscopic Evaluation of Drone Testes During Sexual Maturation

From eclosion (emergence) to sexual maturity, the drone testes decreased in size (i.e., undergo atrophy or involution) on average by 90.9% (SD \pm 0.3%) as assessed by photographed coronal 2D testicular surface area. Seasonal progression affected the rate of testicular atrophy ($F = 39.0$, $df = 1, 7$; $P < 0.05$), with drones emerging in July achieving sexual maturity 3–4 d before drones emerging in June (Fig. 3). Honey bee drones emerged with testes at their greatest size (7.9–10.8 mm²) and subsequently decreased in size to an atrophic end-stage (0.9–1.0 mm²) once sexual maturity was reached between days 9 and 14 postemergence (Figs. 2 and 3). The testicular size of drones reared in July differed significantly from those reared in June starting on day 6 postemergence (Fig. 3).

Microscopic Evaluation of Drone Testes During Sexual Maturation

The macroscopic decrease in testicular size corresponded to a progressive pattern of histological change in the testicular tubules, germ cells, and supporting stroma. The changes were described daily and subsequently divided into four stages based on common, sequential, testicular microscopic morphology during the sexual maturation period (summarized in Table 1). These changes appeared to occur in a continuum, in an order that reflected the relative age of the cells along the tubule, and progressed from a basilar to apical direction, where basilar tubular sections appeared histologically older than their corresponding apical segments. This pattern of apical segments

appearing less mature compared to basilar segments was most prominent for the first two described histologic stages.

Stage I – Conclusion of Spermiogenesis in Follicular Cells (Days 1–3 Postemergence)

The testes were surrounded by a penetrating tracheal mesh (tr, Fig. 4A and C), and abundant perivisceral fat (fb) adjacent to a thin external peritoneal sheath (p), which surrounded hundreds of tightly packed testicular tubules (tu). Each tubule contained an outer monolayer of squamous, inner peritoneal sheath cells (ips, Fig. 4B–E) which circumscribed a layer of follicular cells (fc), with spermatids (st), and spermatozoa (sz) in cytoplasmic cavities called spermatocysts. Spermatodesms (sd, Fig. 4B–E) were oriented toward the basilar tubule with their tails (ta) are imbedded within the follicular cell layer.

There was a mild difference between apical (Fig. 4B and C) and basilar (Fig. 4D and E) testicular tubular segments. Basilar tubular segments contained no spermatids (st) within spermatocysts of follicular cells and contained more spermatodesms (sd) in the lumen. There was a mild reduction in tubular diameter, from ~125 μ m in apical to 100 μ m in basilar region. The vas deferens (vd, Fig. 4A) was empty, containing only scattered occasional spermatodesms.

Stage II – Evacuation of Spermatodesms From Tubular Lumens (Days 4–6 [July] or 4–9 [June])

The tracheal mesh and peritoneum (p, Fig. 5A) appeared thickened as the area of coronal section of the testes decreased. The follicular cells lining testicular tubules were smaller and their round nuclei with prominent single nucleoli were more distinct from cytoplasm than those in Stage 1. The apical tubules (~100 μ m diameter) (Fig. 5B and C) contained spermatodesms (sd) with tails (ta) imbedded in the follicular cells obscuring the border between tubular lumen and tubular wall.

The basilar tubules (~85 μ m diameter) (Fig. 5D and E) have a well-defined luminal space (tu.l) containing spermatodesms, whose tails were not imbedded within follicular cells (fc, Fig. 5). The spermatodesms were travelling into the vas deferens (vd, Fig. 5A) which appeared dilated with tightly packed spermatodesms, and by days 6 to 8 (in July and June respectively) the entire tubular content

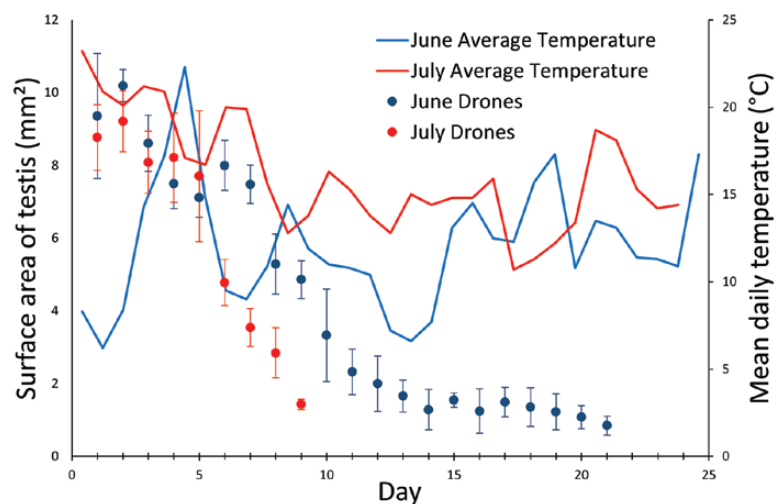


Fig. 3. Sexual maturation of drones and average temperature in June and July, 2017. Sexual maturation was monitored/measured by progressive daily reduction in two-dimensional (coronal) testicular area measured on captured images of dissected formalin fixed drones. The drones were deemed to reach sexual maturity when testicular area was reduced to 2 mm² or less. Sexual maturation of drones was faster in July (warmer days), than in June (colder days) ($P < 0.05$). The graph represents the average surface areas (\pm SD) of each testis of drones ($n = 3$ drones/day) raised in June or July (2017) and daily average temperatures in Saskatoon, SK, Canada over the experimental period (Government of Canada, 2011).

Table 1. Chronological changes during maturation of the testicular parenchyma and supporting structures

Stage	Name	Age (days)		Follicular cells (FC)	Vas deferens
		June	July		
I	Conclusion of spermiogenesis	1–3	1–3	FC contain spermatids (apical only), spermatozoa, and tails of spermatodesms. Indistinct tubular lumen.	Empty
II	Evacuation of spermatodesms from tubular lumens	4–9	4–6	FC do not contain spermatids, or spermatozoa; only tails of spermatodesms. Spermatozoids evacuating basilar tubule.	Packed with spermatodesms
III	Progressive follicular cell atrophy	10–13	7–8	FC do not contain gametes and undergo atrophy. Distinct, empty tubular lumen.	
IV	Complete atrophy and collapse of testicular parenchyma	14+	9+	Complete loss of FC and tubules. Stellate cells, tracheoles, and pigment granules remain.	

The maturation was divided into four phases: conclusion of spermiogenesis, evacuation of spermatodesms from tubular lumens, follicular cell atrophy, and complete atrophy and collapse.

of spermatodesms was transferred into the vas deferens and seminal vesicle.

Stage III – Follicular Cell Atrophy (Days 7–8 [July] or 10–13 [June])

The tracheal mesh and peritoneum (p, Fig. 6A) were thickened, corrugated, and surround markedly reduced testicular parenchyma. Compared to Stage II, the follicular cells lining testicular tubules were 2–3 fold smaller and contained round to oval nuclei (n, Fig. 6B–D) with indistinct nucleoli and denser chromatin. The testicular tubules (~50 µm diameter) (tu, Fig. 6B and C) were lined by low columnar to cuboidal follicular cells with round nuclei in the apical segments whereas in the basilar segments follicular cells were cuboidal to flattened (attenuated) with round to oval nuclei that are affected occasionally by pyknosis (pn, Fig. 6E) or karyorrhexis (* Fig. 6E) consistent with apoptotic processes. The testicular tubules contained only occasional spermatozoa (sz) and no spermatodesms (Fig. 6B–D), whereas vas deferens (vd, Fig. 6A) was distended with spermatodesms.

Stage IV – Complete Atrophy and Collapse (Days 9+ [July] to 14+ [June])

The testes reached the final involution and atrophy with complete loss of tubular parenchyma. The end-stage testes consisted of a collapsed dense tracheal meshwork intermixed with stellate or spindle stromal cells and occasional lipofuscin-laden phagocytic cells (lf, Fig. 7B and C). Grossly, the atrophied testes were triangular and tan – to light green flecks of tissue (~1 mm²), imbedded within a dense tracheal meshwork (Fig. 2B, day 15).

Discussion

This study documented chronological daily histological changes of testes of drones from emergence to sexual maturity during spring and early summer. Light microscopic morphology of testicular changes during sexual maturation was divided into four overlapping stages: Stage I – conclusion of spermiogenesis (day 0–3), Stage II – evacuation of spermatodesms from tubular lumens (day 4–9), Stage III – progressive tubular and follicular cell atrophy (day 7–13), and Stage IV – complete atrophy and collapse of testicular parenchyma (day 9–14). The length of Stages II and III was shortened and sexual maturation of drones accelerated with seasonal progression; namely, drones reared in July matured ~ 4 d earlier than drones reared in June. In addition to chronological morphological differences in testicular histology during sexual maturation, there were also anatomical differences between basilar (closer to vas deferens) and apical (closer to blind end) aspects of testicular tubules. Histological changes affecting follicular cells in basilar segments of tubules were more advanced than those in apical segments.

The detailed histological description of Stages II and III in the current study bridged the gap in the scientific literature and provided the complete chronological light microscopic description of the testicular changes from emergence until sexual maturity of honey bee drones. Previous studies have focused on testicular histology at emergence (Zander 1916, Bishop 1920, Snodgrass and Morse 1956) or after testicular involution, labelled as Stages I and IV, respectively in this study. Recently, Lago et al. (Lago et al. 2020) published a histological atlas illustrating the entire sequential testicular development of honey bee drones during larval, pupal, and pharate stages. Taken together, the work of Lago et al. (Lago et al. 2020) and the current study describe and illustrate the

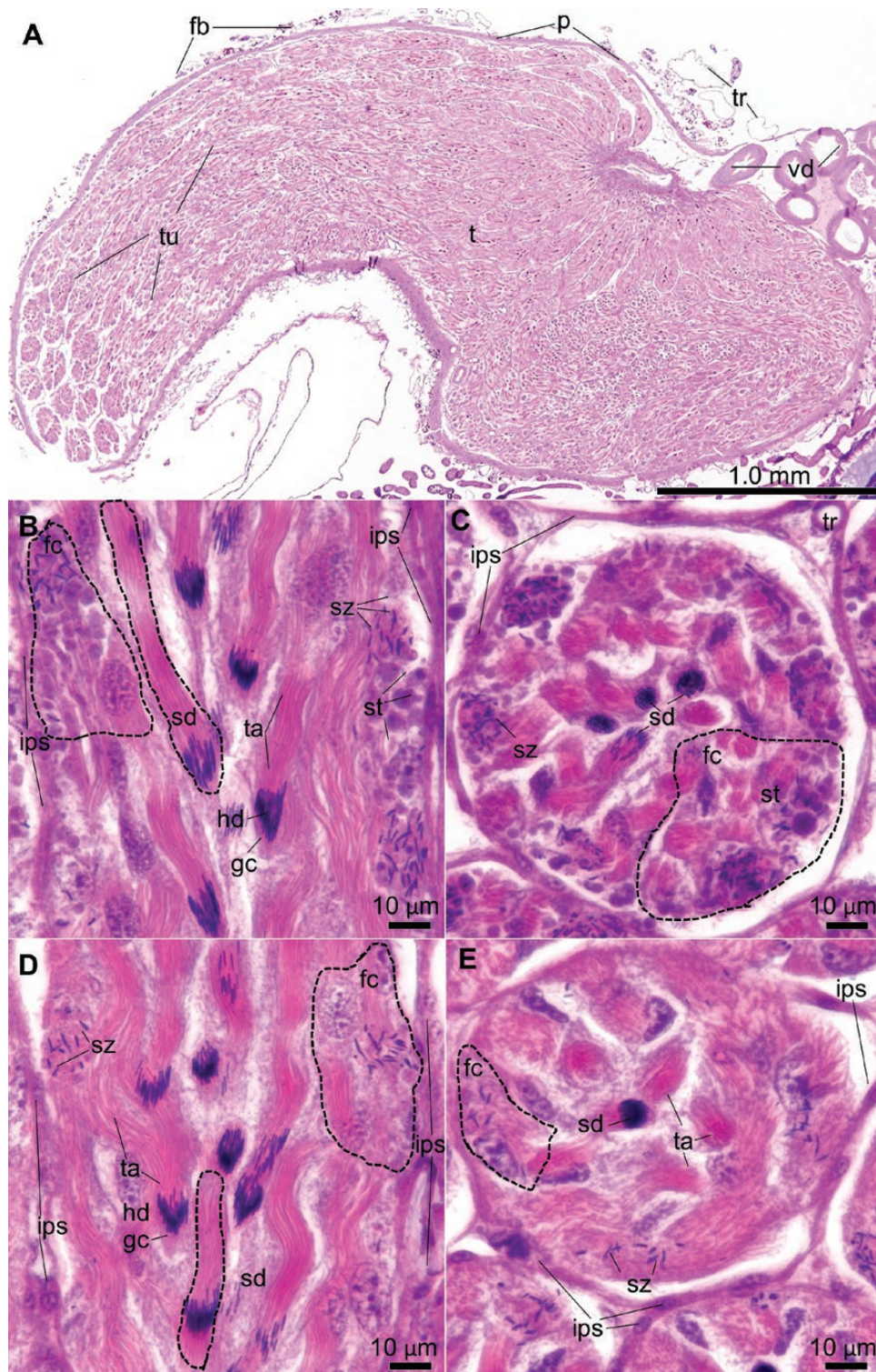


Fig. 4. Stage I – Conclusion of spermiogenesis. Testis of *Apis mellifera* drone at eclosion: (A) Coronal section of vas deferens (vd), testicle (t), and tubules (tu) with surrounding peritoneum (p), visceral fat body (fb), and tracheoles (tr). Longitudinal (B) and cross section (C) of an apical tubule with follicular cells (fc) housing individual spermatids (st) and spermatozoa (sz). Spermatodesms (sd) are oriented basilarly, with heads (hd) and glycoprotein caps (gc) in the lumen and tails (ta) extending apically. The tubule is circumscribed by an inner peritoneal sheath (ips), with external tracheoles (tr). Longitudinal (D) and cross section (E) of a basilar tubule displaying a similar structure with more mature gametes. Spermatodesms (sd) occupying the tubular lumen with heads (hd) and glycoprotein cap (gp) oriented to the vas deferens and tails (ta) associated with the lining follicular cells (fc) which also hold imbedded spermatozoa (sz).

comprehensive histological testicular development of honey bee drones from the third larval instar to complete sexual maturity (9–14 d after emergence).

Microscopic morphological changes in drone testes are correlated with macroscopic progressive reduction in testicular size during sexual maturation. Testicular size plateaus for 3 d after

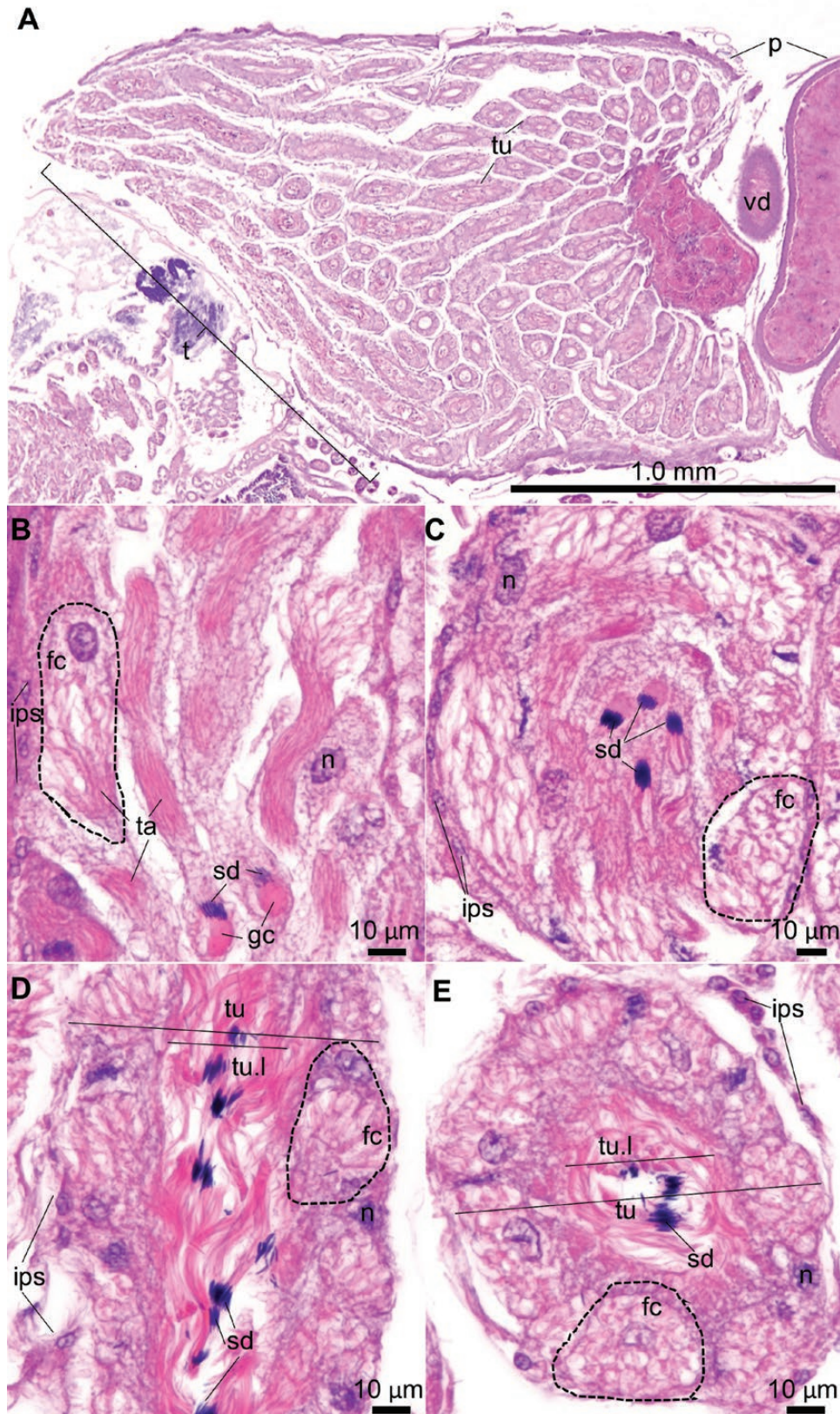


Fig. 5. Stage II – Evacuation of spermatodesms from tubular lumens. Testis and vas deferens of a five-day-old *Apis mellifera* drone. (A) A coronal section of the testicle (t), tubules (tu), vas deferens (vd), and peritoneum (p). A longitudinal (B) and cross section (C) of the apical tubule still releasing formed spermatodesms (sd) with glycoprotein cap (gp) and tails (ta) extending apically or to the follicular cell (fc) cytoplasm (nucleus, n; inner peritoneal sheath, ips). The longitudinal (D) and cross section (E) of the basilar tubules have more empty luminal space as they approach the vas deferens. The tubular lumen (tu.l) becomes more distinct from the follicular cell lining as the former evacuates its spermatodesms. The follicular cells have large vacuoles with eosinophilic flocculent material and deeply staining eosinophilic material lining the luminal surface.

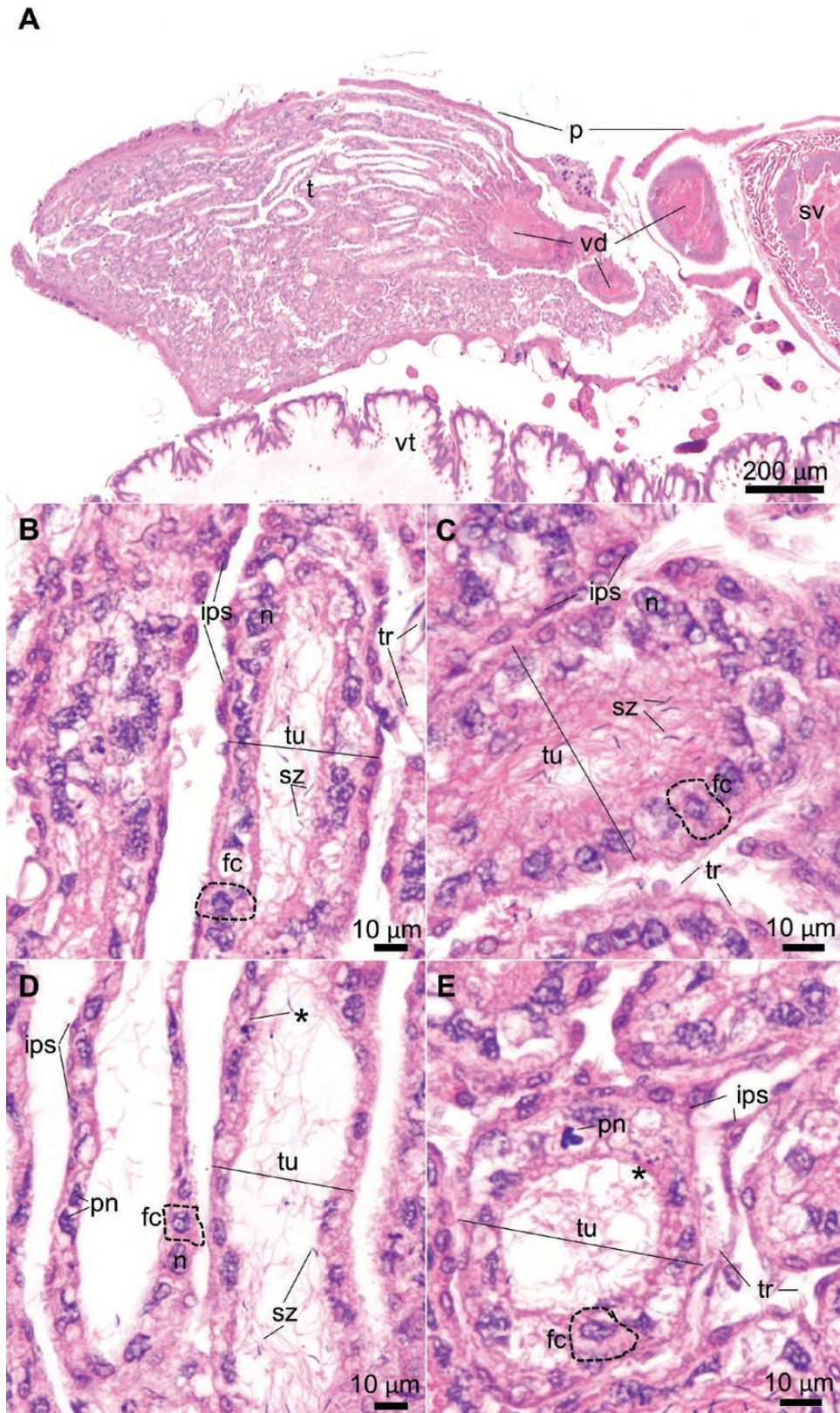


Fig. 6. Stage III – Progressive follicular cell atrophy. Testis (t), vas deferens (vd), seminal vesicle (sv), and adjacent the ventriculus (vt) of a 10-day-old *Apis mellifera* drone. (A) Coronal section of the testicle (t) covered by peritoneum (pt). Longitudinal (B) and cross (C) section of the apical tubules (tu) shows scant individual spermatozoa (sz) and atrophic follicular cells (fc), inner peritoneal sheath (ips), tracheoles (tr), and follicular cell nuclei (n). The basilar tubules (D and E) are mostly empty, with attenuated, hyper-eosinophilic follicular cells with scattered pyknotic nuclei (pn) and karyorrhexis (*).

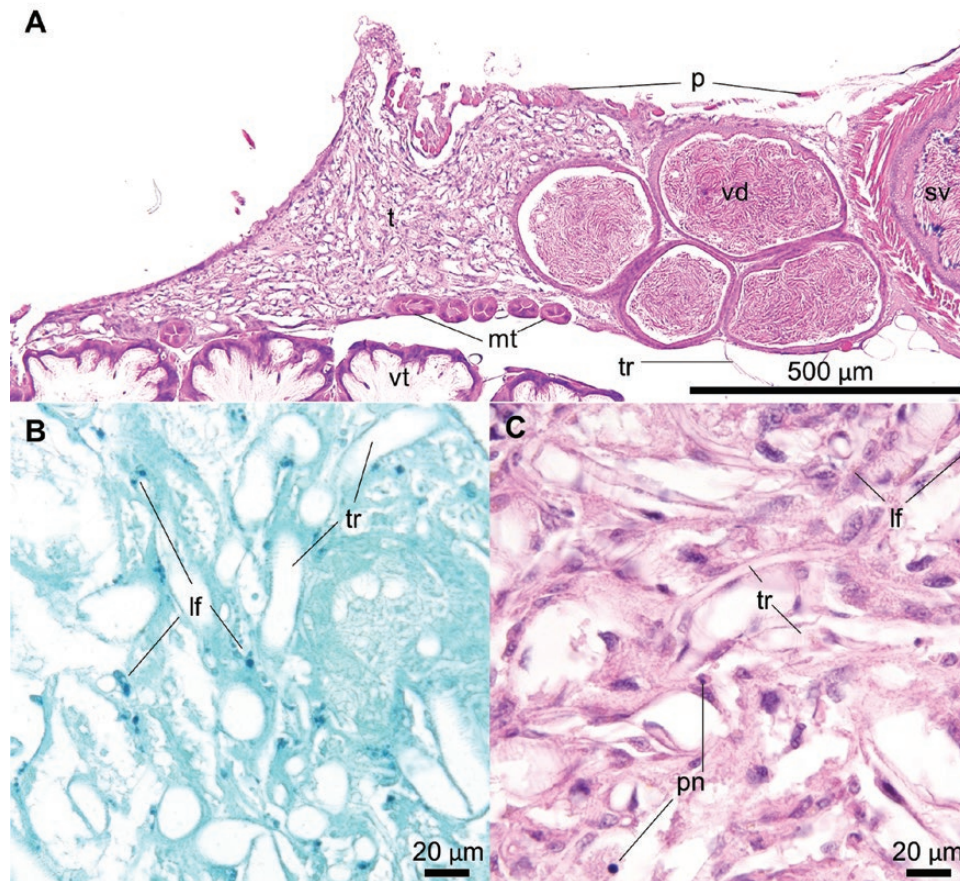


Fig. 7. Stage IV – Complete atrophy and collapse of testicular parenchyma. Testis (t), vas deferens (vd), and seminal vesicle (sv) of a 15-day-old *Apis mellifera* drone. (A) A coronal section of the testicle and vas deferens with abundant tracheal (tr) network within the ruffled peritoneum (p) with adjacent Malpighian tubules (mt) and ventriculus (vt). Schmorl's stain (B) reveals numerous dark green granules consistent with lipofuscin (lf) throughout the testicular remnant. The tubules are no longer distinguishable (C), but the tracheoles (tr) persist with scattered stellate stroma cells with scattered golden-brown pigment, and pyknotic nuclei (pn).

eclosion which corresponds to Stage I of sexual maturation and is characterized by the conclusion of spermiogenesis in follicular cells and accumulation of spermatodesms in tubular lumens. Macroscopic testicular reduction in size begins with Stage II, which is histologically characterized by evacuation of spermatodesms from tubular lumens into vas deferens and seminal vesicles. The final reduction of testicular size occurs during Stage III which consists of progressive atrophy of follicular cells and testicular tubules once the sperm is completely transferred into vas deferens and seminal vesicles. The ‘end-stage’ atrophic and involuted testes occur during Stage IV once follicular cells disappear and testicular tubules collapse and are intermixed with tracheoles and consolidated stroma. Once end-stage testicular atrophy and involution was reached, there were no further macroscopic or microscopic changes until the end of the experiment at day 21.

The histological changes in testes of *A. mellifera* drone observed during sexual maturation in the current study are comparable to those reported in other hymenopteran insects with semelparous mating. Postemergence spermiogenesis (Histological Stage I) observed in the current study is also present in testes of newly emerging Meliponini bees (*Friesella schrottkyi*) and Indian honey bees (*Apis ceranae indica*) (Kapil 1962, Sawarkar and Tembhare 2015), which is followed by transfer of sperm out of testicular tubules (Histological Stage II) (Sawarkar and Tembhare 2015) and disorganization and loss of follicular cells (Histological Stage III) that result

in final testicular atrophy (Histological Stage IV) (Cruz-Landim and Dallacqua 2002, Landim 2008). The end-state (Stage IV) of mature hymenopteran testes is histologically similar across many species and is consistent with our findings in *A. mellifera* drones (Cruz-Landim and Dallacqua 2002, Moors et al. 2009, Allard et al. 2011, Sawarkar and Tembhare 2015). The duration of postemergence sexual maturation of hymenopteran males ranges from 9 to 14 d in *Vespula vulgaris* wasps (Moors et al. 2009), *Friesella schrottkyi* stingless bees (Brito et al. 2010), *Solenopsis invicta* ants (Ball and Vinson 1984), and *Apis ceranae indica* (Sawarkar and Tembhare 2015), which is comparable to *Apis mellifera* drones observed in this study. Other hymenopterans drones display active spermatogenesis at emergence, such as the wasps [*Ancistrocerus antilope* (Bushrow et al. 2006), and *Vespula vulgaris* (Moors et al. 2009)] and ants [*Gnamptogenys bicolor* (Allard et al. 2011)], similar to the pre-emergence testes of the drone (Lago et al. 2020). The latter two organisms (Moors et al. 2009, Allard et al. 2011) show patterns of histological involution similar to those described in this study.

The previously published period for sexual maturation of drones ranges from 6 to 8 d (Bishop 1920, Mackensen and Roberts 1948) to 12–16 d (Winston 1991), which is consistent with the current study. Increased environmental temperature is reported to accelerate drone sexual maturation (Jaycox 1961, Czekońska et al. 2013), which was also observed in this study. Despite the change in maturation rate, the serial presentation of the four histological stages was

maintained. The drones in this experiment were confined within the drone compartment using queen excluder mesh to prevent attrition of free-flying drones; this prevented normal drone behaviour such as orientation and voiding flights during the first couple of weeks after emergence. The effects of confinement stress on experimental drones used in the current experiment are unknown. Nevertheless, the time to reach sexual maturity was within the previously published range (Bishop 1920, Mackensen and Roberts 1948, Winston 1991). Regardless, it may be useful to repeat this study with free-flying drones to rule out potential negative impact of confinement on testicular histological morphology during maturation.

Power et al (Power et al. 2020) recently published an investigation of histopathological changes in testes of 25 free-flying healthy drones, the age of which was estimated according to whole-body mass (Metz and Tarpay 2019). Based on microscopic evaluation, 17/25 drones had normal testicular parenchyma with germ cells within follicular cells and spermatodesms in tubular lumens which correspond to histological Stages I and II, respectively, described in the current study. They also observed degeneration and necrosis of follicular and germ cells within seminiferous (testicular) tubule of 5/25 drones and delayed or incomplete maturation of germ cells in 2/25 drones. Interestingly, Power et al. (Power et al. 2020) also indicated that an experimental histopathological study describing testicular changes during sexual maturation of drones was lacking. The current study fills this gap, and the detailed histological description of testicular changes will enable differentiation of normal atrophic processes occurring during sexual maturation from pathological processes described by Power et al. (Power et al. 2020).

This study describes chronological histological changes of testes obtained from drones with synchronized age from emergence to sexual maturity. Testicular histological changes during sexual maturation of drones were divided into four stages: I – conclusion of spermiogenesis, II – evacuation of spermatodesms from tubular lumens, III – progressive follicular cell atrophy, and IV – complete atrophy and collapse of testicular parenchyma. In addition to chronological morphological differences in testicular histology during progression of sexual maturation, there are also anatomical differences in progression of maturation between apical and basilar segments of testicular tubules. Accordingly, both chronological and anatomical variations in microscopic changes in testes during normal sexual maturations should be considered in future studies investigating potential pathological effects of biotic and abiotic stressor on testes of drones during sexual maturation.

Acknowledgments

We thank Dr. Sophie Derveau for the technical assistance. Financial support was provided by Western Grains Research Foundation (Agricultural Development Fund 20150125, 2016) <http://westerngrains.com/>, Saskatchewan Canola Development Commission (Agricultural Development Fund 20150125, 2016) <http://www.saskcanola.com/>, Saskatchewan Agricultural Development Fund (20160157, 2017) <https://www.saskatchewan.ca/business/agriculture-natural-resources-and-industry/agribusiness-farmers-and-ranchers/agricultural-research-programs/knowledge-creation/agriculture-development-fund>, and Mitacs Accelerate (IT09712) <https://www.mitacs.ca/en>.

References Cited

- Allard, D., F. Ito, Y. Aikawa, A. Gotoh, and J. Billen. 2011. Testes degeneration in ants: a histological study of *Gnamptogenys bicolor*: testes degeneration in the ant *Gnamptogenys bicolor*. *Acta Zoologica*. 92: 372–376.
- Apivar® (amitraz) [package insert]. 2016. Villebon sur Yvette, Île-de-France. Veto-Pharma, France.
- Ball, D. E., and S. B. Vinson. 1984. Anatomy and histology of the male reproductive system of the fire ant, *Solenopsis invicta* Buren (Hymenoptera: Formicidae). *Int J Insect Morphol Embryol*. 13: 283–294.
- Bishop, G. H. 1920. Fertilization in the honey-bee. I. The male sexual organs: their histological structure and physiological functioning. *J Exp Zool*. 31: 224–265.
- Brito, P., U. Zama, H. Dolder, and J. Lino-Neto. 2010. New characteristics of the male reproductive system in the Meliponini bee, *Friesella schrottkyi* (Hymenoptera: Apidae): histological and physiological development during sexual maturation. *Apidologie*. 41: 203–215.
- Bushrow, E. S., C. L. Fuller, D. P. Cowan, and C. A. Byrd. 2006. Anatomy of the male reproductive system and sperm morphology in the caterpillar-hunting wasp *Ancistrocerus antilope* (Hymenoptera, Vespidae). *Invertebr Biol*. 125: 354–362.
- Collins, A. M., T. J. Caperna, V. Williams, W. M. Garrett, and J. D. Evans. 2006. Proteomic analyses of male contributions to honey bee sperm storage and mating. *Insect Mol. Biol*. 15: 541–549.
- Colonello, N. A., and K. Hartfelder. 2003. Protein content and pattern during mucus gland maturation and its ecdysteroid control in honey bee drones. *Apidologie*. 34: 257–267.
- Colonello, N. A., and K. Hartfelder. 2005. She's my girl - male accessory gland products and their function in the reproductive biology of social bees. *Apidologie*. 36: 231–244.
- Cruz-Landim da, C. 2001. Organization of the cysts in bee (Hymenoptera, Apidae) testis: number of spermatozoa per cyst. *Iheringia, Série Zoologia*. 91: 183–189.
- Cruz-Landim da, C., and R. P. Dallacqua. 2002. Testicular reabsorption in adult males of *Melipona bicolor bicolor* Lepeletier (Hymenoptera, Apidae, Meliponini). *Cytologia*. 67: 145–151.
- Czekońska, K., B. Chuda-Mickiewicz, and P. Chorbiński. 2013. The effect of brood incubation temperature on the reproductive value of honey bee (*Apis mellifera*) drones. *J Apic Res*. 52: 96–105.
- Da Cruz-Landim, C., D. Beig, and R. L. M. S. De Moraes. 1980. The process of differentiation during spermatogenesis in bees (Hymenoptera, Apidae). *Caryologia*. 33: 1–15.
- Forbes, J. 1954. The anatomy and histology of the male reproductive system of *Camponotus pennsylvanicus* DeGeer (Formicidae, Hymenoptera). *J Morphol*. 95: 523–555.
- Government of Canada. 2011. Historical data - climate - environment and climate change Canada. Available from https://climate.weather.gc.ca/climate_data/daily_data_e.html?timeframe=2&hlyRange=2008-12-02%7C2020-11-13&dlyRange=2008-12-02%7C2020-11-13&mlyRange=%7C&StationID=47707&Prov=SK&urlExtension=_e.html&searchType=stnProv&optLimit=yearRange&StartYear=2017&EndYear=2018&selRowPerPage=25&Line=80&lstProvince=SK&Day=14&Year=2017&Month=6#.
- Jaycox, E. R. 1961. The effects of various foods and temperatures on sexual maturity of the drone honey bee (*Apis mellifera*). *Ann Entomol Soc Am*. 54: 519–523.
- Kapil, R. P. 1962. Anatomy and histology of the male reproductive system of *Apis indica* FAB (Apidae, Hymenoptera). *Insectes Sociaux*. 9: 73–90.
- Klowden, M. J. 2013. *Physiological systems in insects*. Elsevier, Amsterdam, NL.
- Lago, D. C., J. R. Martins, R. P. Dallacqua, D. E. Santos, M. M. G. Bitondi, and K. Hartfelder. 2020. Testis development and spermatogenesis in drones of the honey bee, *Apis mellifera* L. *Apidologie*. 51: 935–955.
- Landim da, C. C. 2008. *Abelhas: morfologia e função de sistemas*. SciELO – Editora UNESP, São Paulo, BR.
- Luna, L. G., and A. F. I. of Pathology (U.S.). 1968. *Manual of histologic staining methods of the armed forces institute of pathology*. Blakiston Division, McGraw-Hill, New York, NY.
- Mackensen, O., and W. C. Roberts. 1948. *A manual for the artificial insemination of queen bees*. Government Printing Office; U.S. Dept. Agric, Washington.
- Metz, B. N., and D. R. Tarpay. 2019. Reproductive senescence in drones of the honey bee (*Apis mellifera*). *Insects*: 10: 11.
- Moors, L., and J. Billen. 2009. Age-dependent morphology and ultrastructure of the cornua glands in drones of *Apis mellifera*. *Apidologie*. 40: 600–607.

- Moors, L., O. Spaas, G. Koeniger, and J. Billen. 2005. Morphological and ultrastructural changes in the mucus glands of *Apis mellifera* drones during pupal development and sexual maturation. *Apidologie*. 36: 245–254.
- Moors, L., E. Schoeters, K. Coudron, and J. Billen. 2009. Morphological changes in the male accessory glands and testes in *Vespula vulgaris* (Hymenoptera, Vespidae) during sexual maturation. *Invertebr Biol*. 128: 364–371.
- Moors, L., G. Koeniger, and J. Billen. 2012. Ontogeny and morphology of the bulbos, part of the male reproductive organ in *Apis mellifera carnica* (Hymenoptera, Apidae). *Apidologie*. 43: 201–211.
- Oxytet-25® (oxytetracycline-HCL) [package insert]. Medivet Pharmaceuticals, High River, AB, Canada; 2016.
- Power, K., M. Martano, G. Altamura, and P. Maiolino. 2020. Histopathological findings in testes from apparently healthy drones of *Apis mellifera ligustica*. *Vet Sci*. 7: 124.
- Rego do de, L. N. A. A., R. Silistino-Souza, M. T. V. de Azeredo-Oliveira, and L. Madi-Ravazzi. 2013. Spermatogenesis of *Zaprionus indianus* and *Zaprionus sepsoides* (Diptera, Drosophilidae): cytochemical, structural and ultrastructural characterization. *Genet Mol Biol*. 36: 50–60.
- Sawarkar, A. B., and D. B. Tembhare. 2015. Testis morphology and spermatogenesis in the Indian honeybee, *Apis cerana indica* F. (Hymenoptera: Apidae). *J Entomol Zool Stud*. 3: 489–492.
- Shyamalanath, S., and Forbes, J. 1983. Anatomy and histology of the male reproductive system in the adult and pupa of the doryline ant, *Aenictus gracilis* Emery (Hymenoptera: Formicidae). *J N Y Entomol Soc*. 91: 377–393.
- Smith, D. S. 1968. Insect cells: their structure and function. Oliver & Boyd, Edinburgh, UK.
- Snodgrass, R. E. 1910. The anatomy of the honey bee. Government Printing Office; U.S. Dept. Agric. Bur. Ent., Washington, DC.
- Snodgrass, R. E. 1935. Principles of Insect Morphology. McGraw-Hill, New York, NY.
- Snodgrass, R. E. 2018. Principles of insect morphology. Cornell UP, Ithaca, NY.
- Snodgrass, R. E., and R. A. Morse. 1956. Anatomy of the honey bee. Comstock Pub. Associates, Ithaca, NY.
- StataCorp. 2017. Stata 15 base reference manual. Stata Press, College Station, TX.
- Suvarna, K. S., C. Layton, and J. D. Bancroft. 2012. Bancroft's theory and practice of histological techniques: expert consult: online and print. Elsevier Health Sciences, Amsterdam, NL.
- Swammerdam, J. 1738. Biblia naturae: sive, Historia insectorum. *Leydae: Apud Isaacum Severinum, Baldinum Vander Aa, Petrum Vander Aa*.
- Winston, M. L. 1991. The biology of the honey bee. Harvard University Press, Cambridge, MA.
- Woyke, J., and Z. Jasinski. 1978. Influence of age of drones on the results of instrumental insemination of honeybee queen. *Apidologie*. 9: 203–212.
- Woyke, J., and F. Ruttner. 1958. An anatomical study of the mating process in the honeybee. *Bee World*. 39: 3–18.
- Zander, E. 1916. Die Ausbildung des Geschlechtes bei der Honigbiene (*Apis mellifica* L.). *Zeitschrift für Angewandte Entomologie*. 3: 1–6.